Fluid flow in highly porous anisotropic graphites

2002 J. Phys.: Condens. Matter 14 1119

(http://iopscience.iop.org/0953-8984/14/6/301)

INSTITUTE OF PHYSICS PUBLISHING JOURNAL OF PHYSICS: CONDENSED MATTER

J. Phys.: Condens. Matter **14** (2002) 1119–1129 PII: S0953-8984(02)30905-6

Fluid flow in highly porous anisotropic graphites

A Celzard[1] **and J F Marêché**

Laboratoire de Chimie du Solide Minéral, Université Henri Poincaré–Nancy I, UMR-CNRS 7555, BP 239, 54506 Vandoeuvre-lès-Nancy, France

E-mail: Alain.Celzard@lcsm.uhp-nancy.fr

Received 16 November 2001
Published 1 February 2002
Online at stacks.iop.org/JPhysCM/14/1119

Abstract

In a previous work (Celzard A and Marêché J F 2001 *J. Phys.: Condens. Matter* **13** 4387), the properties of transport in the pore space of a sample of expanded graphite compressed to a density of 140 kg m^{-3} were investigated. It was found from gas permeability, ion diffusion and mercury porosimetry that the porous structure could be modelled by cylindrical pores of length l and diameters δ such that $l = \delta$. In this context, the theory of Katz and Thomson (Katz A J and Thompson A H 1986 *Phys. Rev.* B **34** 8179) and that of Johnson *et al* (Johnson D L, Koplik J and Schwartz L M 1986 *Phys. Rev. Lett.* **57** 2564) were both shown to lead to very good agreement between the estimates and the experimental results. In the present paper, these studies are continued for a wide range of highly porous monolithic cubes of different densities. The latter are seen to have strongly porosity-dependent permeabilities (k), formation factors (F) and anisotropies. It is evidenced that the calculation of the formation factors may be achieved from the experimental values of the permeability in the framework of Johnson, Koplik and Schwartz theory, based on the $l = \delta$ model. The calculated values are found to be in good agreement with the measured ones. Also, the expected relationship $k \sim F^{-2}$ is recovered. Hence, it is suggested that the properties of transport in the pore space of such highly porous graphites may be completely accounted for by the above models. Finally, the critical pore radii δ_c as defined by Katz and Thomson are calculated; the theoretical expression $kF \sim \delta_c^2$ is checked with our materials.

1. Introduction

While porous media are obviously characterized by their porosity Φ, their permeability k is also a property of great importance. Indeed, it is easy to find systems having the same porosity but very different transport properties throughout their pore space. The reason lies in the fact that k depends strongly on the porous structure, and especially on the absolute size of the pores and

[1] Author to whom any correspondence should be addressed.

their necks, while Φ is just an adimensional parameter. Thus, a given porous material is really characterized if some cross-property relations between several porosity-dependent quantities are established. Since the 1980s, many theoretical and experimental studies have been carried out in order to find such relationships [1,2]. One of the conclusions which could be drawn from these works is that none of the theories works simultaneously for several different materials. In our opinion, a suitable model of pore structure should be first identified. Once this has been done, a good agreement between the results of the various theories could be obtained. This is what the present paper intends to show.

In a previous work, the transport properties in the pore space of a cubic sample made of expanded graphite (EG) compressed to a density of 140 kg m^{-3} were investigated [3]. In particular, the gas permeability and the formation factor, both anisotropic, were measured. The results were confronted with mercury porosimetry experiments and analysed in the framework of several models, in particular that of Johnson, Koplik and Schwartz [4] (JKS theory). The relationships linking the permeability, the formation factor and the critical pore diameter were also established [3]. The present paper is a continuation of our previous study dealing with this particular sample. Let us first recall that the formation factor F is an adimensional parameter defined in porous systems whose pore space is saturated with a conducting fluid (i.e., a liquid electrolyte). F characterizes the effective resistance to current flow throughout the material and may be measured either by ion diffusion experiments or derived from electrical conductivity measurements. However, the latter method requires that the solid phase is not conducting. The formation factor reads $F = \sigma_0/\sigma = D_0/D$, where σ_0 and D_0 are the conductivity and the diffusion coefficient corresponding to the free electrolyte, respectively, while σ and D are standing for those of the saturated pore space of the material. Unlike the permeability k, the parameter F is a scale-invariant quantity, meaning that if the sizes of the pores and that of the solid grains are magnified or shrunk, leaving the porosity unchanged, its values are unaffected. The critical pore diameter δ_c, as defined by Katz and Thomson [5, 6], is derived from mercury injection experiments. δ_c is the length scale at which the invading mercury first forms a connected path spanning the sample. It was shown in [3] that the model of pore structure assuming cylindrical pores of length l and diameter δ such that $l = \delta$ was the only one which was consistent with the various experimental results for k, F and δ_c.

In this paper, attempts are made to extent the above findings to a series of highly porous monolithic graphites made by compression of EG into cubes of various densities. The materials are described in section 2, and their permeabilities and formation factors are given in section 3. The results are shown to be correctly accounted for by the JKS theory in the framework of the pore structure model $l = \delta$. In other words, the conclusions first derived in the case of a given sample of compressed EG are shown to apply to the whole set of available materials. Moreover, despite a strong anisotropic character and unusually low permeabilities and high formation factors, the expected relationship $k \sim F^{-2}$ is observed in section 4. Finally, the critical pore diameter is calculated for each porosity, and its links with both k and F are checked with the available experimental data.

2. Experimental procedure

2.1. Compressed expanded graphite samples

Production of highly porous (and most of the time anisotropic) graphitic materials is readily achieved by compressing a given variety of EG. The latter consists of worm-like particles of about 1.5 cm in length, having a density of 15 kg m^{-3} and a surface area close to 40 m^2 g^{-1}. Its industrial production consists in rapid heating of residue compounds of natural graphite flakes with sulphuric acid [7]. The brutal volatilization of the intercalate induces a huge unidirectional

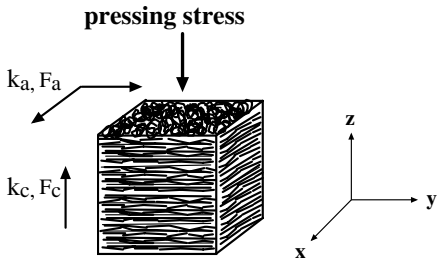

Figure 1. Definition of two orthogonal directions of measurement for both the permeability k and the formation factor F. a is the direction parallel to the bedding plane of the graphite flakes (xy-plane), i.e., normal to the pressing stress, whereas c is the one perpendicular to the bedding plane (z-axis), i.e., parallel to the pressing stress.

expansion of the initial particles, and hence highly porous 'accordions' of graphite are obtained. Scanning electron microscopy shows that their microstructure is roughly that of a flattened irregular honeycomb network of graphite [8–11]. Raw EG is thus a very light material, having in the present case an apparent density of 7.5 kg m^{-3}. One striking feature of its particles is their ability to be mechanically interlocked into each other by simple compression. Thus, autoconsolidated highly porous monoliths of pure graphite may be easily obtained without binder [12].

A series of monolithic cubes was prepared just like in our previous study, i.e., by uniaxial compaction of EG. Such consolidated blocks are characterized by apparent densities ranging typically from 50 up to 300 kg m^{-3}. Then, assuming a bulk density of 2200 kg m^{-3} for pure graphite, this means that the corresponding porosities are as high as about 86–98%. Preparing such materials by uniaxial compression obviously induces orientation of the constituting graphite flakes. Indeed, as expected, the samples described above were already shown to exhibit anisotropic conducting and elastic properties [13–15]. In this context, it should be recalled that compressed EG is a transverse isotropic material. Thus, two orthogonal directions of measurement, termed a and c, may be defined as shown in figure 1. Consequently, the permeabilities and the formation factors will be measured below along these two directions.

2.2. Measuring permeabilities and formation factors

The devices used for the measurements of the permeability k and the formation factor F of cubic porous samples of compressed EG have been described elsewhere [3]. Briefly, for measuring k_a and k_c, nitrogen is forced to flow throughout the sample along the xy-plane (see figure 1) and along the z-axis, respectively. Measuring simultaneously the inlet pressure P and both the pressure drop over the sample and the flow rate allows one to calculate the permeability for the direction considered. The experiment is repeated for several values of P; then k is extrapolated to the limit of infinite pressure using Klinkenberg's equation [3, 16]. k has the dimension of an area but, most of the time, it is given in units of darcies or millidarcies, where 1 millidarcy $\approx 10^{-15}$ m^2. With nitrogen flowing throughout the samples used in this study (thickness 2 cm, cross-sectional area 4 cm^2) under a pressure gradient of 1 atm, 1 millidarcy corresponds to a flow rate of about 0.11 cm^3 s^{-1}.

In figure 2, the permeabilities of the blocks are presented on a logarithmic scale as a function of their porosity Φ. It is seen that k is isotropic for the highest values of Φ, while it becomes increasingly anisotropic as the porosity decreases. As stated above, such behaviour is not surprising since it was already observed for both electrical conductivity and elastic moduli [13–15]. Indeed, these properties are anisotropic as soon as the densities of the

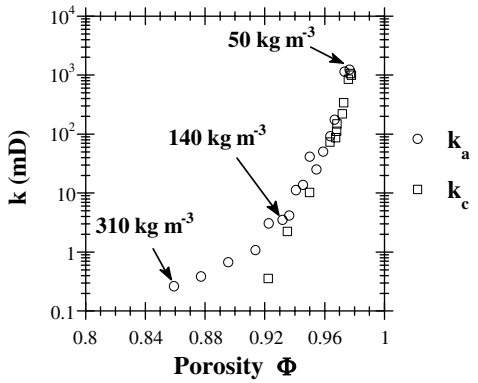

Figure 2. Permeabilities (k) of the samples of compressed EG as a function of their porosity (Φ). A few corresponding densities are given in the figure. ('mD' is standing for millidarcies.)

materials are greater than about 50 kg m^{-3}, i.e., for porosities lower than 98%. The present results provide evidence that the isotropic or anisotropic character exhibited by the properties of the pore space is tightly linked to that of the graphite backbone.

Another striking feature of figure 2 is that the permeability drops very quickly as the porosity decreases. Thus, for $\Phi \approx 0.98$, the greatest value obtained for k is close to 1 darcy, while k is about 1000 times lower for $\Phi \approx 0.92$. These permeabilities are rather low for such high porosities. Indeed, it is interesting to compare the values of k in compressed EG with what has been measured for other common materials. Such data were gathered by Scheidegger [17]: either the permeabilities of most of these media are similar, but for much lower porosities (e.g., in sandstones, $k \approx 0.5$–3000 millidarcies for $\Phi \approx 0.08$–0.38), or, for similar porosities, the corresponding permeabilities are much higher than in compressed EG (e.g., in fibreglass, $k \approx 2.4 \times 10^4$ to 5.1×10^4 millidarcies for $\Phi \approx 0.88$–0.93). In other words, the values of k presented here are much lower and vary much more quickly than in any other porous systems.

The formation factors $F_{a\,(c)}$ are defined as $D_0/D_{a\,(c)}$, where D_0 is the diffusion coefficient of given ions in a solvent, and $D_{a\,(c)}$ their diffusion coefficients within the pores of the samples along the directions a (c). Again, details of the experimental conditions and the set-up were already given in a previous work [3]. Briefly, the materials are carefully impregnated with water laced with wetting agents, and a 1 M copper sulphate aqueous solution is allowed to diffuse throughout them. The diffusion coefficients are then derived from ionic conductivity measurements, which are performed as a function of time (the results are presented in figure 3). Unfortunately, because of a lack of EG deriving from the original batch, fewer samples were available for formation factor measurements than permeability measurements. Again, just like for k, the comparison with what may be found in the literature shows that the values of F are high in compressed EG in view of its very large porosity. For example, many systems such as consolidated packings of grains exhibit formation factors close to 10 for porosities close to 0.2 [18–20].

3. Theoretical aspects and discussion

3.1. Permeability variations over the entire range of porosity

For any porous system, the behaviour of the permeability depends on the range of porosity considered. Typically, there are three regions of Φ wherein k follows different expressions, as shown in figure 4 which is for a packing of spherical solid grains.

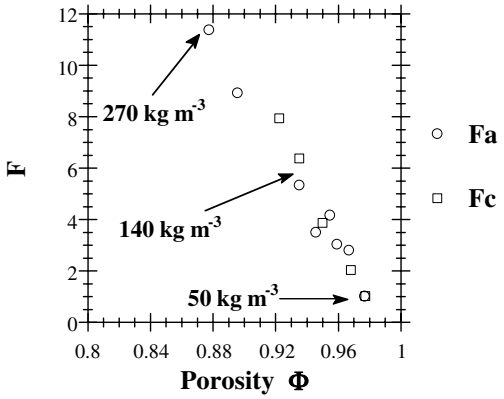

Figure 3. Formation factors (F) of the samples of compressed EG as a function of their porosity (Φ). A few corresponding densities are given in the figure.

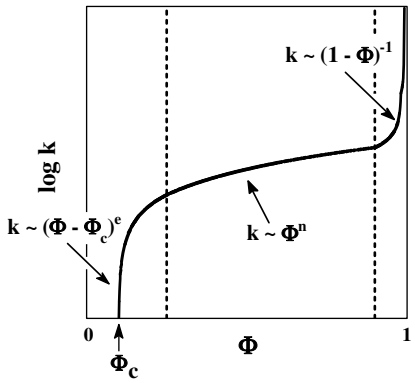

Figure 4. Typical theoretical variations of the permeability (k) of a porous system made of spherical grains, as a function the (intergranular) porosity (Φ). The percolation threshold corresponds to the critical porosity Φ_c at which k vanishes. Three porosity ranges in which the permeability is non-zero may be defined (see the text).

In the low-porosity range, a percolation behaviour is expected close to the permeability threshold Φ_c. Thus,

$$k \sim (\Phi - \Phi_c)^e \tag{1}$$

where e is a critical exponent whose value is close to 2 in any three-dimensional classical system [21]. The permeability does in fact vanish at a critical value of Φ, for which a fluid is no longer able to flow throughout the porous system. In rocks, Φ_c may be as low as a few per cent [22, 23], while it amounts typically to 15% in materials for which the porosity is achieved by dissolving one phase randomly dispersed in an insoluble matrix [24]. Foils made of highly compressed EG are widely used as seals and gaskets [25, 26]; moreover, this material is known to be impervious for densities as low as 1100 kg m^{-3} [27], proving that the permeability threshold is such that $\Phi_c \geqslant 0.5$. To our knowledge, so remarkably high a critical porosity has never been observed in any other material.

In the intermediate-porosity range, the old and well known empirical relationship (see [16, 17, 23] and references therein)

$$k \sim \Phi^n \tag{2}$$

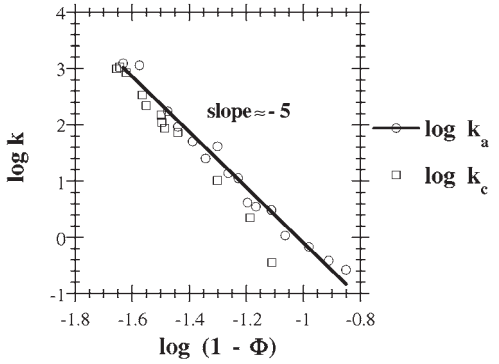

Figure 5. Observation of the empirical law $k \sim (1-\Phi)^{-5}$ for compressed EG over the whole range of porosities studied.

(which has been also confirmed by effective-medium theory [23]) is usually observed. n is an empirical exponent, often close to 3 in 3D systems [19, 28]; however, n is sometimes found to take other values, ranging typically from 1.5 to 8.5 [29]. Such variation is probably due to the fact that materials having different porosities may have very different permeabilities, depending on their porous structure.

Finally, in the high-porosity range, k tends to infinity as the porosity becomes 100%. For a Stokes flow around a dilute suspension of spheres, the following rigorous result may be obtained [30]:

$$k \sim \frac{1}{1-\Phi}. \tag{3}$$

Clearly, our samples of compressed EG correspond to the high-porosity range, because neither of the relationships (1) and (2) is observed. While $\Phi \to 1$, the permeability increases even faster than what is suggested by equation (3). Indeed, the plot of $\log k$ versus $\log(1-\Phi)$ leads to a straight line whose slope is close to -5, as shown in figure 5. Therefore, an empirical law such as $k \sim (1-\Phi)^{-5}$ could apply over the whole range of porosities studied in the case of k_a, and at least for the highest values of Φ for k_c. It will be shown below that such rapid changes of permeability as a function of the porosity are related to simultaneous variations of the formation factor and the interconnected pore size.

3.2. Calculation of the formation factors

As recalled above, the theory of Johnson, Koplik and Schwartz [4] (referred to as JKS theory), applied to the model of porous structure with $l = \delta$, was shown to work correctly for a sample of compressed EG having a density of 140 kg m^{-3} [3]. In this context, the permeability was shown to read

$$k = c\frac{\Lambda^2}{8F} \tag{4a}$$

where c is a constant and Λ a length scale measuring the dynamically interconnected pore size [1, 31]. According to Banavar and Johnson [32], the constant c which must be used in the $l = \delta$ model is

$$c = 27\frac{(1+t)^{3+t}}{(3+t)^{3+t}} \approx 2.07 \tag{4b}$$

where the parameter t is the critical exponent for the electrical conductivity ($t \simeq 1.9$ in most three-dimensional systems [33]).

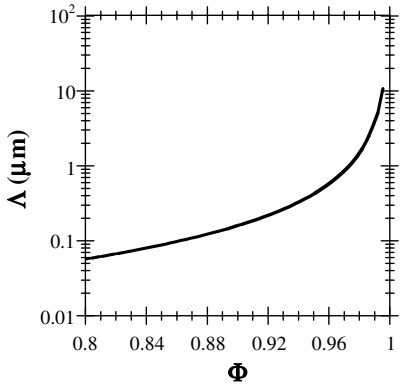

Figure 6. Interconnected pore size Λ calculated as a function of the porosity of the compressed EG blocks.

Many porous media having porosities such that $0.40 < \Phi < 1.00$ are modelled by packings and suspensions of spherical grains. In these systems, the parameter Λ obeys the following equation [4]:

$$\Lambda = \frac{2\Phi d}{9(1-\Phi)} \tag{5}$$

where d is the grain diameter. Even though this model is very rough in the case of compressed EG, it can be checked and compared with the available experimental results. Thus, a kind of effective diameter $d_{(\Phi)}$ could be attributed to the EG particles, whose densities $\rho_{(\Phi)}$ are calculable for each porosity of the resultant monoliths [34]. Now, for a sphere

$$d_{(\Phi)} = \sqrt[3]{\frac{6m}{\pi\rho_{(\Phi)}}} \tag{6}$$

where m is the mass of the grain. Since m is not known *a priori*, calculating the absolute values of Λ requires additional data. For the sample of density 140 kg m^{-3}, the formation factors were calculated on two bases: in one case, in the framework of JKS theory for the $l = \delta$ model of pore structure, and, in the other case, using the experimental permeability values [3]. The corresponding Λ was thus found to be 0.304 μm, very close to the value derived just from the surface area and the pore volume of the same material (0.289 μm).

Hence, Λ is now calculated for each porosity from equations (5) and (6), and from the density data whose calculation is detailed in [34], in such a way that $\Lambda_{(140\,\mathrm{kg\,m^{-3}})} = 0.304\ \mu$m. The results are given in figure 6, as a function of the porosity of the compressed EG blocks. Subsequently, the formation factors may be derived by application of equation (4) using the experimental values of the permeability (given in figure 2) and the calculated values of Λ (see figure 6). Thus,

$$F_{a\,(c)} = 2.07\frac{\Lambda^2}{8k_{a\,(c)}}. \tag{7}$$

The results are presented in figure 7; it may be seen that the formation factors are undervalued at the highest porosities considered. Indeed, by definition of F, any value lower than 1 is unphysical. Finding such low results is probably due to the fact that a model of sphere packing is not suitable for describing compressed EG at very high porosities. However, as shown below, the other calculated values of F agree with the other experimental data.

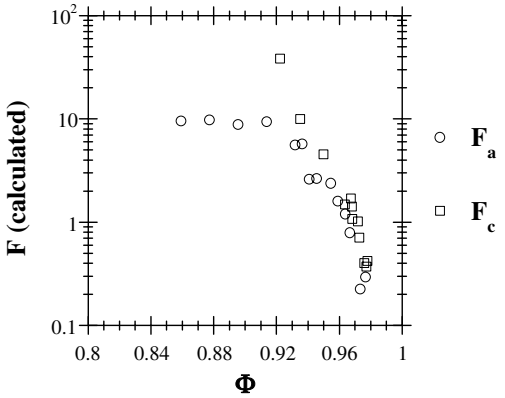

Figure 7. Formation factors calculated from figures 2 and 6 by application of equation (7).

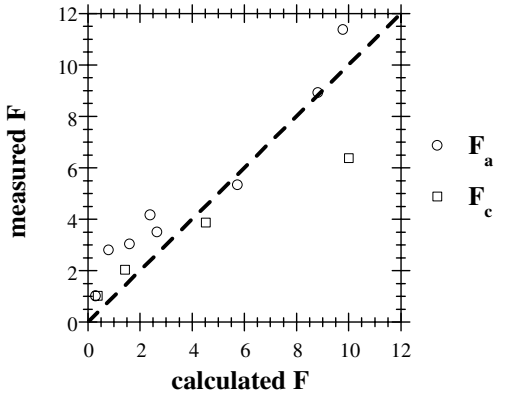

Figure 8. Measured formation factors versus calculated ones. The broken straight line is just a guide for the eye.

- The first evidence showing that most of the calculated values of the formation factors were accurate comes obviously from the direct comparison between calculation and experiment. This is achieved in figure 8, in which both calculated and measured factors F are plotted as functions of each other. The agreement is quite satisfactory over the whole range of porosities studied.
- Also, both the calculated and experimental values of the formation factors strongly support the following theoretical expectations.

4. Permeabilities versus formation factors and pore diameters

4.1. Relationships between permeability and formation factor

The effective conductivity σ of porous media saturated with a conducting fluid is experimentally observed to follow the so-called Archie law [35]. It reads

$$\sigma \sim \sigma_0 \Phi^{n'} \tag{8}$$

where σ_0 is the conductivity of the saturating fluid and n' is an empirical exponent, sometimes referred to as the 'cementation index' [36]. The value of n' in 3D systems is often close to 1.5,

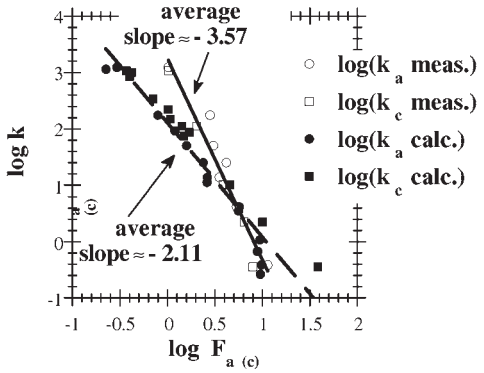

Figure 9. Checking of equation (9) linking the measured permeabilities and the formation factors, either calculated or measured.

but depends on the material (see [19] and references therein). Moreover, in a dilute assembly of spheres, $n' = 3/2$ exactly [28]. Equation (8) was shown to work for a great number of porous materials, and was explained on the basis of percolation theory [37]. Since the formation factor is $F = \sigma_0/\sigma$, then, according to (8), $\Phi \sim F^{-1/n'}$. Substituting equation (2) in (8), one gets $k \sim F^{-n/n'}$. It was shown and confirmed by several experimental studies that $n = 2n'$, both in 2D and in 3D [19]. Hence

$$k \sim F^{-2}. \tag{9}$$

Such a relationship is indeed borne out by the calculated values of F, as shown in figure 9 where $\log k$ is plotted against $\log F$. For both directions of measurement, straight lines are obtained with an average slope of -2.11. It might be remarked that, in the case of compressed EG samples, neither equation (2) nor (8) applies, while equation (9) does. Hence, the experimental validity of the relationship (9) could be fortuitous. However, it is also possible that the range of application of equation (9) is wider than those of (2) and (8), and thus that (9) is 'more universal' than the other dependences.

If $\log k$ is now plotted against $\log F$ using the experimentally measured formation factors, a power law just like equation (9) is observed, but with a greater exponent. Indeed, the average slope accounting for the two directions of measurement is close to -3.5. However, the range of values of F with which the linear fit is made is smaller than the previous one, dealing with calculated values. Therefore, given the scattering of the experimental points, it is not easy to reach a conclusion about an effective deviation of equation (9). Moreover, putting together on the same plot both experimental and calculated versions of $\log F$ versus $\log k$ leads to a set of data points which may be fitted by a straight line with a slope of -2.17 and a correlation coefficient of 0.94.

4.2. Porosity-dependent critical pore diameters

A link between Katz and Thomson [5, 6] and JKS theories has been established by Banavar and Johnson [32] in the framework of the $l = \delta$ model. It reads

$$\Lambda = \frac{\delta_c}{2(1+t)} \tag{10}$$

where δ_c and t have the same meaning as before. Thus, it is possible to calculate the values of the critical pore diameters from equation (10) and from the results for Λ given in figure 6. Combining equations (7) and (10), one obtains

$$F_{a\,(c)} k_{a\,(c)} = 7.68 \times 10^{-3}\, \delta_c^2. \tag{11}$$

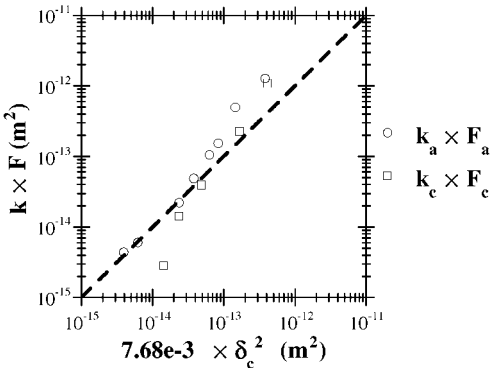

Figure 10. Checking of equation (11), according to which the product permeability multiplied by the formation factor is proportional to the squared critical pore diameter δ_c. The broken straight line is just a guide for the eyes.

Such an expression may be checked with compressed EG, using fully independent data, i.e., the experimental values of both F and k, and the calculated values of δ_c. Figure 10 shows that equation (11) is obeyed well. This provides evidence that the critical pore diameters δ_c, and hence the interconnected pore sizes Λ, were rather accurately calculated on the basis of our assumptions about the densification of EG.

5. Conclusions

The anisotropic permeabilities k and formation factors F of a series of highly porous cubes of compressed EG were measured. It was shown that both quantities were strongly porosity-dependent, k being rather low and F rather high, considering the very high relative pore volumes of the materials. From the experimental data of k, calculated values of F could be obtained in the framework of JKS theory based on a particular pore model. In the latter, the pores are seen as capillary tubes whose lengths l and diameters δ were such that $l = \delta$. Comparison between measured and calculated factors F proved that JKS theory is very efficient as long as a suitable pore model is first identified (the $l = \delta$ model in our case). Also, the expected relationship linking permeabilities and formation factors, $k \sim F^{-2}$, was recovered. On the basis of a rough model of sphere packing, the interconnected pore size Λ was calculated for each porosity. From these values, the critical pore diameter δ_c of KT theory has been derived. Finally, the relationship $kF \sim \delta_c^2$, on which much theoretical work is based [1,5,6,32,38–41], was checked with our materials.

Hence, the conclusions derived from the careful study of a single material were found to be relevant for the series of samples. Thus, since a suitable pore model has been identified for compressed EG, it seems that the properties of its pore space are completely characterized now. Indeed, the cross-property relations between the various quantities discussed in this paper (k, F, Λ, δ_c) are fully identified, at least for the range of porosities studied. Measuring two properties among the four allows one to derive the others, based on the equations given in this paper.

Acknowledgments

The authors are grateful for the financial support of ECODEV-CNRS through the GDRE 'Adsorbants Carbonés et Environnement' and the Council of the Région Lorraine.

References

[1] Schwartz L M, Martys N, Bentz D P, Garboczi E J and Torquato S 1993 *Phys. Rev.* E **48** 4584
[2] Torquato S 1994 *Physica* A **207** 79
[3] Celzard A and Marêché J F 2001 *J. Phys.: Condens. Matter* **13** 4387
[4] Johnson D L, Koplik J and Schwartz L M 1986 *Phys. Rev. Lett.* **57** 2564
[5] Katz A J and Thompson A H 1986 *Phys. Rev.* B **34** 8179
[6] Katz A J and Thompson A H 1987 *J. Geophys. Res.* **92** 599
[7] Inagaki M and Suwa T 2001 *Carbon* **39** 915–20
[8] Stevens R E, Ross S and Wesson S P 1973 *Carbon* **11** 525
[9] Klatt M, Furdin G, Hérold A and Dupont-Pavlovsky N 1986 *Carbon* **24** 731
[10] Yoshida A, Hishiyama Y and Inagaki M 1991 *Carbon* **29** 1227
[11] Inagaki M and Nakashima M 1994 *Carbon* **32** 1253
[12] Dowell M B and Howard R A 1986 *Carbon* **24** 311
[13] Celzard A, Marêché J F, Furdin G and Puricelli S 2000 *J. Phys. D: Appl. Phys.* **33** 3094
[14] Krzesiñska M, Celzard A, Marêché J F and Puricelli S 2001 *J. Mater. Res.* **16** 606
[15] Celzard A, Krzesiñska M, Marêché J F and Puricelli S 2001 *Physica* A **294** 283
[16] Dullien F A L 1979 *Porous Media—Fluid Transport and Pore Structure* (New York: Academic)
[17] Scheidegger A E 1974 *The Physics of Flow through Porous Media* 3rd edn (Toronto: University of Toronto Press)
[18] Kostek S, Schwartz L M and Johnson D L 1992 *Phys. Rev.* B **45** 186
[19] Wong P, Koplik J and Tomanic J P 1984 *Phys. Rev.* B **30** 6606
[20] Schwartz L M and Banavar J R 1989 *Phys. Rev.* B **39** 11 965
[21] Sahimi M 1994 *Applications of Percolation Theory* (Bristol, PA: Taylor and Francis)
[22] Knackstedt M A and Cox S F 1995 *Phys. Rev.* E **51** R5181
[23] Sahimi M 1995 *Flow and Transport in Porous Media and Fractured Rocks* (Weinheim: VCH)
[24] Shelekhin A B, Dixon A G and Ma Y H 1993 *J. Membrane Sci.* **83** 181
[25] Chung D D L 1987 *J. Mater. Sci.* **22** 4190
[26] Chung D D L 2000 *J. Mater. Eng. Perform.* **9** 161
[27] Carbone-Lorraine Group (France) 1990 Papyex, flexible graphite *Technical Paper*
[28] Groupe Poreux P C 1987 *Phys. Scr.* T **19** B524
[29] Hilfer R 1993 *Physica* A **194** 406
[30] Berryman J G and Blair S C 1986 *J. Appl. Phys.* **60** 1930
[31] Kostek S, Schwartz L M and Johnson D L 1992 *Phys. Rev.* B **45** 186
[32] Banavar J R and Johnson D L 1987 *Phys. Rev.* B **35** 7283
[33] Fisch R and Brooks Harris A 1978 *Phys. Rev.* B **18** 416
[34] Celzard A, Schneider S and Marêché J F 2001 *Carbon* submitted
[35] Archie G E 1942 *Trans. AIME* **146** 54
[36] Sen P N, Scala C and Cohen M H 1981 *Geophysics* **46** 781
[37] Balberg I 1986 *Phys. Rev.* B **33** 3618
[38] Le Doussal P 1989 *Phys. Rev.* B **39** 4816
[39] Avellaneda M and Torquato S 1991 *Phys. Fluids* A **3** 2529
[40] Saeger R B, Scriven L E and Davis H T 1991 *Phys. Rev.* A **44** 5087
[41] Garboczi E J 1990 *Cement Concrete Res.* **20** 591